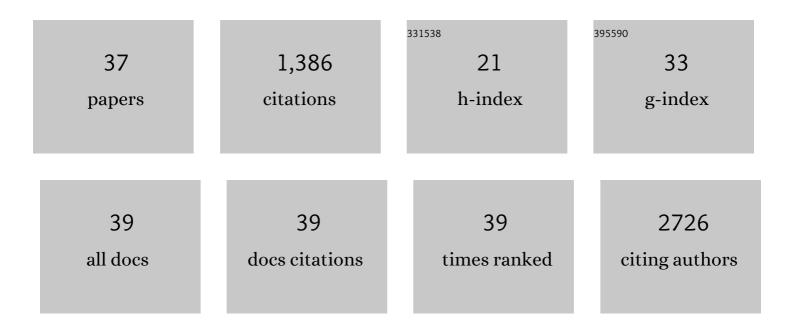
Andrea Urbani

List of Publications by Year in descending order

Source: https://exaly.com/author-pdf/1997017/publications.pdf Version: 2024-02-01



ANDREA HORANI

#	Article	IF	CITATIONS
1	Repurposing of Trimetazidine for amyotrophic lateral sclerosis: A study in SOD1 ^{G93A} mice. British Journal of Pharmacology, 2022, 179, 1732-1752.	2.7	21
2	Identification of biomarkers for physical frailty and sarcopenia through a new multi-marker approach: results from the BIOSPHERE study. GeroScience, 2021, 43, 727-740.	2.1	37
3	Defining the molecular mechanisms of the mitochondrial permeability transition through genetic manipulation of F-ATP synthase. Nature Communications, 2021, 12, 4835.	5.8	52
4	Insight into the mechanism of cytotoxicity of membrane-permeant psoralenic Kv1.3 channel inhibitors by chemical dissection of a novel member of the family. Redox Biology, 2020, 37, 101705.	3.9	22
5	A novel multi-marker discovery approach identifies new serum biomarkers for Parkinson's disease in older people: an EXosomes in PArkiNson Disease (EXPAND) ancillary study. GeroScience, 2020, 42, 1323-1334.	2.1	32
6	Mitochondrial Ion Channels of the Inner Membrane and Their Regulation in Cell Death Signaling. Frontiers in Cell and Developmental Biology, 2020, 8, 620081.	1.8	24
7	Molecular nature and regulation of the mitochondrial permeability transition pore(s), drug target(s) in cardioprotection. Journal of Molecular and Cellular Cardiology, 2020, 144, 76-86.	0.9	54
8	Circulating amino acid signature in older people with Parkinson's disease: A metabolic complement to the EXosomes in PArkiNson Disease (EXPAND) study. Experimental Gerontology, 2019, 128, 110766.	1.2	32
9	Purified F-ATP synthase forms a Ca2+-dependent high-conductance channel matching the mitochondrial permeability transition pore. Nature Communications, 2019, 10, 4341.	5.8	139
10	Arg-8 of yeast subunit e contributes to the stability of F-ATP synthase dimers and to the generation of the full-conductance mitochondrial megachannel. Journal of Biological Chemistry, 2019, 294, 10987-10997.	1.6	32
11	Proteomic and metabolomic characterization of streptozotocin-induced diabetic nephropathy in TIMP3-deficient mice. Acta Diabetologica, 2018, 55, 121-129.	1.2	25
12	A Distinct Pattern of Circulating Amino Acids Characterizes Older Persons with Physical Frailty and Sarcopenia: Results from the BIOSPHERE Study. Nutrients, 2018, 10, 1691.	1.7	82
13	The cristae modulator Optic atrophy 1 requires mitochondrial ATP synthase oligomers to safeguard mitochondrial function. Nature Communications, 2018, 9, 3399.	5.8	111
14	Direct Pharmacological Targeting of a Mitochondrial Ion Channel Selectively Kills Tumor Cells InÂVivo. Cancer Cell, 2017, 31, 516-531.e10.	7.7	138
15	Perturbations in cell signaling elicit early cardiac defects in mucopolysaccharidosis type II. Human Molecular Genetics, 2017, 26, 1643-1655.	1.4	34
16	MicroRNAs-Proteomic Networks Characterizing Human Medulloblastoma-SLCs. Stem Cells International, 2016, 2016, 1-10.	1.2	8
17	Comparison of Different Matrices as Potential Quality Control Samples for Neurochemical Dementia Diagnostics. Journal of Alzheimer's Disease, 2016, 52, 51-64.	1.2	18
18	Systems biology analysis of the proteomic alterations induced by MPP+, a Parkinson's disease-related mitochondrial toxin. Frontiers in Cellular Neuroscience, 2015, 9, 14.	1.8	24

Andrea Urbani

#	Article	IF	CITATIONS
19	Liver protein profiles in insulin receptor-knockout mice reveal novel molecules involved in the diabetes pathophysiology. American Journal of Physiology - Endocrinology and Metabolism, 2015, 308, E744-E755.	1.8	10
20	An integrated metabolomics approach for the research of new cerebrospinal fluid biomarkers of multiple sclerosis. Molecular BioSystems, 2015, 11, 1563-1572.	2.9	65
21	Proteomic analysis of human sonic hedgehog (SHH) medulloblastoma stem-like cells. Molecular BioSystems, 2015, 11, 1603-1611.	2.9	34
22	Inductive proteomics and large dataset collections. Molecular BioSystems, 2015, 11, 1485-1486.	2.9	1
23	Propofol protects against opioid-induced hyperresponsiveness of airway smooth muscle in a horse model of target-controlled infusion anaesthesia. European Journal of Pharmacology, 2015, 765, 463-471.	1.7	25
24	Calcium and voltage imaging in arrhythmia models by high-speed microscopy. , 2014, , .		0
25	High speed microscopy techniques for signaling detection in live cells. Proceedings of SPIE, 2014, , .	0.8	0
26	Multispot multiphoton Ca2+ imaging in acute myocardial slices. Journal of Biomedical Optics, 2014, 20, 1.	1.4	4
27	Metabolomics signature improves the prediction of cardiovascular events in elderly subjects. Atherosclerosis, 2014, 232, 260-264.	0.4	133
28	l-Carnitine status in end-stage renal disease patients on automated peritoneal dialysis. Journal of Nephrology, 2014, 27, 699-706.	0.9	19
29	Loss of TIMP3 exacerbates atherosclerosis in ApoE null mice. Atherosclerosis, 2014, 235, 438-443.	0.4	46
30	A metaproteomic pipeline to identify newborn mouse gut phylotypes. Journal of Proteomics, 2014, 97, 17-26.	1.2	14
31	The Mitochondrial Italian Human Proteome Project Initiative (mt-HPP). Molecular BioSystems, 2013, 9, 1984-92.	2.9	10
32	Multispot two-photon imaging of calcium waves dynamics in cardial tissue at 16Hz frame rate. Proceedings of SPIE, 2013, , .	0.8	0
33	Detection of calcium waves in mice heart tissue with multispot two-photon imaging. , 2013, , .		0
34	TIMP3 Overexpression in Macrophages Protects From Insulin Resistance, Adipose Inflammation, and Nonalcoholic Fatty Liver Disease in Mice. Diabetes, 2012, 61, 454-462.	0.3	66
35	Proteomic profiling of ATM kinase proficient and deficient cell lines upon blockage of proteasome activity. Journal of Proteomics, 2012, 75, 4632-4646.	1.2	20
36	Toward personalized hemodialysis by low molecular weight amino-containing compounds: future perspective of patient metabolic fingerprint. Blood Transfusion, 2012, 10 Suppl 2, s78-88.	0.3	17

#	Article	IF	CITATIONS
37	Role of different voltage-gated Ca ²⁺ channels in cortical spreading depression: Specific requirement of P/Q-type Ca ²⁺ channels. Channels, 2011, 5, 110-114.	1.5	37